Mesenchymal stromal cells attenuate pulmonary fibrosis via macrophage

Zan Tang
Shenzhen Institutes of Advanced Technology Chinese Academy of Sciences
Junxiao Gao
Shenzhen Institutes of Advanced Technology Chinese Academy of Sciences
Jie Wu
Shenzhen Beike biotechnology
Guifang Zeng
Shenzhen Beike biotechnology
Yan Liao
Shenzhen Beike biotechnology
Zhenkun Song
Shenzhen Beike biotechnology
Xiao Liang
Shenzhen Beike biotechnoloy
Junyuan Hu
Shenzhen Beike biotechnology
Yong Hu
Shenzhen Institutes of Advanced Technology Chinese Academy of Sciences
Muyun Liu (liumuyun@nlelpct.com)
National-local associated engineering laboratory for personalized cell therapy
Nan Li
Shenzhen Institutes of Advanced Technology Chinese Academy of Sciences

Research Article

Keywords: human umbilical cord mesenchymal stem cell, single cell RNA sequencing, macrophage, regulatory T cell

Posted Date: April 30th, 2021

DOI: https://doi.org/10.21203/rs.3.rs-465985/v1

Version of Record: A version of this preprint was published at Stem Cell Research & Therapy on July 13th, 2021. See the published version at https://doi.org/10.1186/s13287-021-02469-5.

Abstract

Background Pulmonary fibrosis (PF) is a growing clinical problem with limited therapeutic options. Human umbilical cord mesenchymal stromal cell (hucMSC) therapy is being investigated in clinical trials for the treatment of PF patients. However, little is known about the underlying molecular and cellular mechanisms of hucMSC therapy on PF. In this study, the molecular and cellular behavior of hucMSC was investigated in a bleomycin induced mouse PF model.

Methods: The effect of hucMSC on mouse lung regeneration was determined by detecting Ki67 expression and Edu incorporation in alveolar type 2 (AT2) and lung fibroblast cells. The hucMSC was transfected to express the membrane localized GFP before transplant into the mouse lung. The cellular behavior of hucMSC in mouse lung was tracked by GFP staining. Single cell RNA sequencing was performed to investigate the molecular mechanism of hucMSC on PF.

Results: hucMSCs could alleviate collagen accumulation in lung and decrease the mortality of mouse induced by bleomycin. hucMSCs transplantation promoted AT2 cell proliferation and inhibited lung fibroblast cell proliferation. Mouse lung macrophage phenotype was changed after interacting with hucMSCs. By using single-cell RNA sequencing, a subcluster of interferon-sensitive macrophages were identified after hucMSC infusion. These macrophages elevate the secretion of CXCL9 and CXCL10 following hucMSC infusion and recruit more Treg cells to the injured lung.

Conclusions: Our study establishes a link between hucMSCs, macrophage proliferation, and PF with potential applications in PF therapeutics. It provides new insights into how hucMSCs interact with macrophage during the repair process of bleomycin-induced PF and play its immunoregulation function.

Introduction

Pulmonary fibrosis (PF) is a chronic progressive disease that happens when lung damaged and scarred due to an aberrant wound-healing process (Martinez et al., 2017). The thickened, stiff scar tissue makes blood oxygenation difficult and results in shortness of breath (Downey, 2011). Numerous factors cause PF, including exposure to certain toxins, tobacco smoke, medical conditions, radiation therapy, viral infection, and some medications (Baumgartner et al., 1997; Liu et al., 2013; Sheng et al., 2020). Mouse genetic studies suggest that lung epithelial cells, especially alveolar type 2 cells, play a key role in initiating the pathogenic process and excessive pulmonary fibroblast proliferation and extracellular matrix (ECM) deposition leads to the destruction of alveolar structure (Barkauskas et al., 2013; Wu et al., 2020; Yao et al., 2021).

Pulmonary macrophages contain two populations: alveolar macrophages (AMs) which reside in the alveolar lumen and interstitial macrophages (IMs) that are located in the lung parenchymal tissue (Kopf et al., 2015; Tan and Krasnow, 2016). Macrophages are crucial regulators of PF and undergo phenotypic and functional changes during the initiation, maintenance, and resolution phases following lung injury

(Aran et al., 2019; Byrne et al., 2016; Wynn and Vannella, 2016). AMs are involved in ECM processing through the secretion of matrix metalloproteases (Atabai et al., 2009; Dancer et al., 2011). In the bleomycin-induced PF mouse model, IMs acquired a pro-fibrotic phenotype with increased expression of CD206 (a mannose receptor) during the fibrotic phase (Ji et al., 2014; Misharin et al., 2013).

The role of mesenchymal stromal cells (MSCs) in the treatment of PF has been investigated in several studies (Jun et al., 2011; Lee et al., 2010; Ortiz et al., 2003). MSC therapy has shown beneficial effects in animal experimental PF models by their potential immunosuppressive and anti-inflammatory activities (Moodley et al., 2009; Ono et al., 2015). However, the detailed cellular and molecular mechanisms of MSCs in PF treatment remain to be elucidated.

In this work, we found that MSCs interact with macrophages and recruit regulatory T cells (Tregs) in damaged lungs. By using single-cell RNA sequencing, we identified a subtype of interferon-sensitive macrophage with elevated *Cxcl10* expression levels. The increased CXCL10 in macrophages recruits Tregs to the lungs and in turn, suppresses the immune response in the lungs. Our study provides new insights into how MSCs interact with macrophage during the repair process of bleomycin-induced acute injury and play its immunoregulation function.

Methods

Mice

8~12-week-old C57BL/6 mice were purchased from the Guangdong Medical Laboratory Animal Center.

Preparation of hucMSCs

Institutional review board approval from the ShenZhen Integrated Cell Bank was obtained for all procedures. Fresh umbilical cords were collected for scientific study from informed and consenting healthy donor. Mesenchymal tissue was scraped from Wharton's jelly after blood vessels were removed. After cutting into pieces, the tissue was centrifuged at 600 x g for 10 min at room temperature. The tissue was then washed with 0.9% saline solution and cultures at 37°C with 5% CO_2 in serum-free Dulbecco's modified Eagle's medium (DMEM). The primary hucMSCs were obtained after 10 days of culture. P4 hucMSCs were used in this study.

Bleomycin-induced mouse PF model

8~12-week-old mice were anesthetized with isoflurane and received a single endotracheal dose of bleomycin sulfate (2U/kg) at day 0. Treated mice received a single i.v. (tail vein) dose of hucMSCs (5 x 10^5) at day 0.

Measurement of hydroxyproline levels

Lungs lobes were weighed, homogenized, and incubated in 6 M HCl at 110°C for 2 to 6 h. Absorbance at 560 nm was measured and adjusted according to standard curves.

Tissue harvest and fixation

Mice were euthanized with i.p. injection of isoflurane. Mice were dissected to expose the diaphragm and the hearts were perfused with 0.9% saline through the right ventricle. The lungs were inflated to 25 cm H_20 pressure with 4% paraformaldehyde (PFA) and were continually fixed in 4% PFA at 4°C for 24 h. For H&E staining (see below), lungs were embedded in paraffin. For immunolabeling (see below), lungs were submerged in 30% sucrose for 24 h and embedded in O.C.T. medium.

Hematoxylin and Eosin (H&E) staining

The H&E staining followed the basic protocol. Slides were dewaxed and rehydrated. Nuclei were stained by hematoxylin (Phygene, PH0516) for 4 min and the cytoplasm was stained by eosin (Phygene, PH0516) for 3 min. Slides were dehydrated in ascending alcohol solutions and cleared with xylene.

Immunostaining

15 mm thick sections were used for immunostaining. In brief, sections were blocked in 3% BSA/0.1% Triton X-100/PBS for 1 h at room temperature after O.C.T. was removed with PBS. Primary antibodies were diluted in blocks and incubated at 4°C overnight. The following primary antibodies were used: Chicken anti-GFP antibody (Abcam, ab13970, 1:500); Rabbit anti-Prospc (Millipore, ab3786, 1:500); Rat anti-Ki67 (ebioscience, 14-5698-82, 1:200); Rat anti-F4/80 (BioRad, MCA497GA, 1:200). The sections were washed with 3%BSA/0.1% Tween-20/PBS 3 times, then sections were incubated with secondary antibodies in blocks for 3 h at room temperature. All of the secondary antibodies were diluted in blocks at 1:400 dilutions.

Lung dissociation for flow cytometry

Lungs were perfused with saline to remove the blood cells, then inflated intratracheally with 1.5 ml enzyme solution containing neutral protease (Worthington-Biochem, catalog#LS02111, 5U/ml), Collagenase Type I (Gibco, catalog#17100-017, 200U/ml), elastase (Worthington, catalog#2294, 4U/ml), DNase I (Roche, catalog#10104159001, 0.33U/ml) and soaked in the same solution for 45 min at room temperature. The digested lung tissues were gently torn into small pieces and shaken in Dulbecco's modified Eagle medium (DMEM, Gibco) containing 10% FBS for 10 min at room temperature. After filtering through 100 mm and 40 mm strainers, centrifuged cells were incubated with 10 mL red blood cell lysis buffer to remove red blood cells. After centrifugation, cells were resuspended in DMEM for staining and FACS analysis.

Edu proliferation assay

For assessing cell proliferation *in vivo*, Edu (Thermo Fisher Scientific, Catalog#E10415) was administered to mice by intraperitoneal injection at 50 mg of EdU per kg of the mouse (weighed 24 h prior to sacrifice). EdU incorporation was detected using the Click-iT EdU Alexa Fluro 488 flow cytometry assay kit (Invitrogen, catalog#C10632).

Immunostaining for flow cytometry & FACS

For AT2 EdU proliferation assays, cells were fixed and permeabilized by using fixation and permeabilization solutions (BD biosciences, catalog#51-2090KZ). For lung fibroblast proliferation assays, cells were stained with EPCAM, CD45, and CD31. EdU staining was performed by using the Click-iT EdU Alexa Fluro 488 flow cytometry assay kit according to the manufacturer's instructions.

qRT-PCR

Total RNA was extracted from lungs using the RNeasy mini kit (QIAGEN, catalog#74104) according to the manufacturer's instructions. cDNA was made using M-MLV reverse transcriptase (Invitrogen, catalog#28025-013). qRT-PCR was performed using SYBR Green Realtime PCR Master Mix (TOYOBO, catalog#QPK-201).

Live animal imaging

hucMSCs were labeled with the XenoLight DiR (1,1'-dioctadecyltetramethyl-indotricarbocyanine iodide; 'DiR,' Perkin Elmer, Catalog#125964) for 25 min at 37°C at a concentration of 15 mM in PBS. Following labeling, cells were washed twice in 0.9% saline solution to remove unbound dye before i.v. injection. Mice were imaged with a NightOWL *in vivo* imaging system.

Macrophage and hucMSCs co-culture

hucMSCs ($1 \times 10^4/cm^2$) were seeded in a 24 well plate 24 h before co-culture. Macrophages were sorted from the mice lung 1 day after bleomycin treatment and co-cultured with hucMSCs (10:1). The hucMSCs and macrophages were cultured in RPMI-1640, 10% FBS, and 1% Penicillin/Streptomycin. mRNA was extracted after co-culture for 72 h.

Single-cell RNA sequencing

Lung single-cell suspensions were made according to the protocol described above (Lung dissociation for flow cytometry) and then processed following the 10X genomics protocol. We used the Seurat R package (version 3.2.3) as the tool for downstream data analysis and processing. Cells less than 300 expression genes were removed and genes that were not expressed in any cells were excluded. To safeguard against undetected doublets, we kept cells with UMIs < 60000. Also, we removed the cells with high expression of mitochondrial and ribosomal genes (according to the proportion of mitochondria and ribosomes in the gene-barcode matrix, 25% and 1% for mitochondria and ribosomes, respectively). Considering the large

range of UMI counts for each cell, we normalized the UMI counts. We used the log normalization method to normalize the UMI of cell i on gene j by the formula:

$$norm\ \ UMI_{(i,j)} = \log\left(\frac{UMI_{(i,j)}}{\sum_i UMI} \times 10000\right.$$

For dimensionality reduction and clustering analyses, we scaled our normalized UMI data by the formula:

$$scale\ \ UMI_{(i,j)} = \frac{UMI_{(ij)} - \mu}{\sigma}$$

where m and s are the mean and standard deviation of UMIs in cell i, respectively. The two methods are integrated into the Seurat R package.

Before clustering analysis, we reduced the dimension of the gene-barcode matrix. To capture biological signals from the single-cell data, we selected the top 2000 high variation genes according to the variance stabilizing transformation (VST) method and performed the principal component (PC) analysis among them. We selected the top 20 PCs by evaluating the standard deviation across PCs. We used the top 20 PCs for clustering analysis and visualization.

In cluster analysis, we constructed a shared nearest neighbor graph based on k-nearest neighbors calculated from the 20 PCs of the scaled data (k = 20) and used the Louvain algorithm as a modularity function optimizer to determine the number of clusters (resolution: 0.5).

Differential expression analysis

The differentially-expressed genes between one cell group and other cell groups were analyzed by running the Wilcoxon Rank-Sum test. We set the average log fold change threshold to 0.25 and limited the expression of genes > 10% in the two compared cell groups. Genes with FDR-adjusted P values < 0.05 were retained.

Cell type annotation & macrophage screening

After determining the differentially expressed genes of each group of cells, we annotated the cell types based on the top 20 genes with log-fold changes in each group of cells. We referred to the manually curated resource of cell markers database CellMarker, the cell type markers database PanglaoDB.

To ensure the accuracy of the selected macrophages, we conducted two rounds of clustering and differential gene analysis. Cells with high expression levels of T cell markers (*Trbc2*, *Cd3d*, and *Cd3e*) and B cell makers (*Igkc* and *Ighm*) were excluded. Finally, we selected genes with an average log fold change > 0.5 and < -0.5 to do the GO (GO_BP, GO_MF, and GO_CC) and KEGG analysis and retained the GO and KEGG terms in which *p*-adjusted values were < 0.05 as final results.

Statistics

All data are presented as mean ± s.d. (as indicated in figure legends). Experimental analyses were not blinded. Unless otherwise mentioned, most of the data presented in figure panels are based on at least three independent experiments. We used two-tailed Student's *t*-tests to assess differences between means. *p*-values were depicted as follows: *$p < 0.05$; **$p < 0.01$; ***$p < 0.001$.

Results

Mesenchymal stromal cells can ameliorate bleomycin-induced PF

To evaluate the role of human umbilical mesenchymal stromal cells (hucMSCs) on PF, mice were administered a single dose of bleomycin (2U/kg) intratracheally on day 0 (Figure 1A). Concurrent with bleomycin instillation, treatment groups were transplanted a single dose of hucMSCs via tail vein injection. Histologic evaluation of lung tissue from mice at 7, 14, and 21 days after bleomycin treatment revealed that hucMSCs can attenuate bleomycin-induced PF (Figure 1B). Consistent with the lung histology results, collagen content was lower in hucMSCs transplanted mice lungs at 14 and 21 days compared to the bleomycin group (Figure 1C). Furthermore, hucMSCs transplanted mice were more resistant to bleomycin-induced lung injury and exhibited a significant decrease in mortality relative to the bleomycin group (Figure 1D). These results demonstrated that hucMSCs can ameliorate bleomycin-induced PF.

hucMSCs promote lung regeneration after bleomycin treatment

PF is associated with impaired alveolar type 2 (AT2) cell proliferation which can inhibit the repair of the damaged epithelium (Sisson et al., 2010; Yao et al., 2021). To determine if hucMSCs administration affects AT2 proliferation *in vivo*, we stained hucMSCs transplanted mouse lung and bleomycin treated mouse lung groups with the cell proliferation marker Ki67 and AT2 cell marker SPC. On day 7 after bleomycin treatment, we found that a greater number of SPC positive cells were stained with Ki67 in hucMSCs transplanted lungs than in lungs instilled with bleomycin (Figure 2A-2B). Similarly, flow cytometry revealed a significant increase in Edu incorporation in AT2 of hucMSCs transplanted lungs at day 7 compared to bleomycin-instilled lungs (Figure 2C-2D). The abnormal proliferation of lung fibroblasts contributes to the initiation and progression of PF. However, lung fibroblasts are heterogeneous and consist of multiple subtypes such that there is no consensus on a lung fibroblast marker (Xie et al., 2018). Therefore, we used $Epcam^{-}CD31^{-}CD45^{-}$ cells to represent lung fibroblasts in our subsequent studies by excluding lung epithelial cells (Epcam+), endothelial cells (CD31+), and hematopoietic cells (CD45+), respectively. To assess the proliferation of fibroblasts in lungs, we quantified Edu incorporation in $Epcam^{-}CD31^{-}CD45^{-}$ cells on day 7 following bleomycin instillation. After hucMSCs transplantation, the lung fibroblast proliferation rate was lower on day 7 compared to the control group (Figure 2E-2F). However, the AT2 and fibroblast proliferation rates were not different between the hucMSCs-transplanted group and the control group at day 14 post bleomycin instillation (Figure S1A-1C). The AT2 and lung fibroblast proliferation data showed that hucMSCs promoted the

alveolar stem repair process and inhibited abnormal lung fibroblast proliferation which contributed to the attenuation of bleomycin-induced PF.

hucMSCs interact with macrophage in mouse lung after infusion

To investigate how hucMSCs function *in vivo*, we tracked the behavior of hucMSCs by labeling them with a live cell dye, DiR. DiR-labeled hucMSCs aggregated in the lung soon after hucMSCs injection without notable differences between mice treated with saline and bleomycin, and almost all hucMSCs were eliminated from the mice within 7 days in both groups (Figure S2A). To track the behavior of hucMSCs in greater detail, hucMSCs were transfected with membrane green fluorescent protein (mGFP) via lentivirus. Many mGFP-labeled cells were observed in lung sections on day 1, but were far less abundant at day 3 after injection and were absent at day 7 which was consistent with the DiR results (Figure 3A). It has been shown that mesenchymal stromal cells can modulate macrophage phenotypes and were phagocytosed by macrophages in other model systems. To determine if hucMSCs interacted with macrophages *in vivo* after infusion, we co-immunolabeled the lungs with antibodies against the macrophage marker F4/80 as well as GFP. This analysis showed that the hucMSCs were engulfed and phagocytosed by macrophages (Figure 3B). We next investigated the effect of phagocytosing hucMSCs on macrophages. To this end, markers related to macrophage phenotypes were assessed on days 7 and 14. *Nos2*, *Cxcl9*, and *Cxcl10* expression levels were dramatically elevated in mice that received hucMSCs compared to mice treated with bleomycin on day 7 (Figure 3C-3E). Meanwhile, *Mrc1*, *Arg1*, *Chil3*, and *Tgm2* expression levels were significantly decreased at day 14 following hucMSCs injection (Figure 3F-3I). These results suggested that hucMSCs were phagocytosed by macrophages after their infusion which also led to a change in macrophage phenotype.

Single-cell RNA sequencing revealed a novel subtype of interferon-sensitive macrophages after hucMSCs infusion

To gain mechanistic insight into the effects of hucMSCs on macrophages, we performed single-cell RNA-sequencing analysis to characterize the gene expression profiles of lung macrophages 7 days after treatment with either intratracheal bleomycin or hucMSCs infusion, when lung regeneration is active. We analyzed profiles of 1845 total macrophages from all samples with sufficiently high gene expression signals after filtering, normalization, and removal of potential outliers (Figure 4A). We identified six macrophage clusters through unbiased clustering in both treatments (Figure 4B) and all clusters expressed macrophage-specific markers, including *Adgre1*, *Lyz2*, and *CD68* (Figure S3A). All six detected clusters were detected at varying levels in both bleomycin-treated and hucMSC-treated mice: Cluster 0, Cluster 1, Cluster 3, and Cluster 4 were present in bleomycin-treated and hucMSC-treated mice lungs at a relatively similar frequency. On the other hand, Cluster 2 and Cluster 5 were enriched in hucMSC-treated mice lung, especially for Cluster 2 cells in which hucMSCs -treated lungs have a 10-fold increase compared to bleomycin-treated lungs by day 7 (Figure 4C). Cluster 0 was enriched for the expression of fibrosis-associated genes (*Spp1*, *Gpnmb*, *Mmp12*, and *Timp2*). Cluster 1 macrophages expressed high levels of antigen presentation-associated genes (*H2-Eb1*, *H2Ab1*, and *H2Aa*). Macrophages in cluster 3

highly expressed *F13a1*, *Hp*, and *Gsr*, which suggests that Cluster 3 belongs to the monocyte subtype. Macrophages from Cluster 4 expressed genes involved in the inflammatory response, cytokine production, and matrix metalloproteinase activation (*Car4*, *Ctsk*, *Chil3*, *S100a1*, and *Wfdc21*). Cluster 5 macrophages express high levels of the transcription factors *Nr4a1* and *Pou2f2*, which suggests they are the Ly6C^{lo} monocytes (Figure 4D and 4E). Cluster 2 macrophages in particular expressed a strong type 1 IFN (interferon) signature, including the IFN-responsive genes (IRGs) *Rsad2*, *Isg15, Ifit1*, *Ifit2*, *Ifit3*, *Ifi205*, *Irf7*, and *Ly6c2* (Figure 4F), and other IRGs were also highly expressed in IFNSMs (herein referred to as "IFN-sensitive macrophages"). Based on the ontology analysis of marker gene expression, IFNSMs were different from other macrophage clusters. Thus, our analysis demonstrated the emergence of a unique IFNSM cluster in mouse lungs following hucMSCs infusion.

hucMSCs promote interferon responsive gene expression in macrophages

Our observation of the emergence of IFNSMs after hucMSCs infusion encouraged us to examine the relationship between hucMSCs infusion and IFNRMs. To better understand how hucMSCs regulate macrophage behavior, we isolated CD45+; F4/80+ macrophages from mice treated with bleomycin after one day by FACS and co-cultured these cells with hucMSCs (Figure 5A). After three days of co-culture, the expression level of interferon responsive genes significantly increased in macrophages co-cultured with hucMSCs (Figure 5B). This suggested that the direct interaction between hucMSCs and macrophages elevated interferon responsive gene expression in macrophages. To investigate the function of IFNSMs, we analyzed the characteristic genes according to their expression level and subcellular locations. We found that CXCL10 was the most highly expressed secretory protein in the IFNSMs (Figure 5C). Meanwhile, *Cxcl9* and *Cxcl10* were also increased in the macrophages after co-culturing with hucMSCs (Figure 5D). CXCL10 is involved in cell proliferation, migration, and angiogenesis (Karin and Razon, 2018). The receptor of CXCL10 is CXCR3, which is highly expressed in the regulatory T cells (Treg) (Groom and Luster, 2011; Li et al., 2020). To verify whether there was an increased number of Tregs in mice after hucMSCs infusion, we compared the numbers of Tregs in mice treated with bleomycin and hucMSCs on day 7. Flow cytometry indicated that there were more FOXP3 Tregs in hucMSCs injected mice lung (Figure 5E-5F). These data suggest that hucMSCs induced the increase of *Cxc10* expression in macrophages and enhance the recruitment of Tregs to the lungs (Figure 5G).

Discussion

In this study, we found that hucMSCs infusion could ameliorate bleomycin-induced PF. Though hucMSCs disappeared rapidly in the lungs following intravenous administration, hucMSCs still exerted therapeutic effects such as decreased collagen deposition and mortality. hucMSCs were phagocytosed by macrophages and altered their phenotype in the lungs and a unique macrophage cluster that sensitive to interferons was identified by single cell RNA-sequencing. This might be due to the phagocytosis of MSCs changing the sensitivity of macrophages to interferons. The phagocytosis of MSCs by macrophages is consistent with previous reports. The phagocytosis of MSCs changed the transcriptional profile of macrophages and, surprisingly, propagated the function of MSCs despite MSCs no longer being present

in vivo. In the graft versus host disease model, macrophages engulf apoptotic MSCs and produce indoleamine 2,3-dioxygenase, which then performs its immunosuppressive function (Galleu et al., 2017). MSCs could also transfer mitochondrial and microRNA into the macrophage and enhance the bioenergetics of macrophage (Ko et al., 2020; Morrison et al., 2017). Macrophages can also engulf cytoplasmic components of MSCs which might downregulate genes involved in antigen presentation and suppress the activation of helper T cells (Court et al., 2020). MSC-derived exosomes could change the proportion of infiltrating classical and nonclassical monocytes in the lungs after bleomycin treatment and revert the PF (Mansouri et al., 2019; Morrison et al., 2017). The coronavirus disease 2019 (COVID-19) pandemic is caused by severe acute respiratory syndrome coronavirus 2 (SARS-CoV-2). Considering its immunosuppressive ability, MSC-based therapies have been used to alleviate the acute lung injury caused by the virus. Clinical data have shown promising results that MSCs can decrease the mortality of COVID-19 ICU patients (Sanchez-Guijo et al., 2020). MSCs might perform their function with the same mechanism that we observed in the bleomycin-induced mouse model and promote damage repair processes after COVID-19 infection.

CXCL9 and CXCL10 are chemokines of the CXC subfamily, whose main function is promoting the trafficking of various leukocytes and mobilizing lung mesenchymal progenitor cells, regulating angiogenesis, and vascular remodeling (Strieter et al., 2007). CXCL10-deficient mice have dramatically increased fibroblast accumulation and more severe PF (Jiang et al., 2010; Tager et al., 2004). The deficiency of the CXCL9 and CXCL10 receptor, CXCR3, also causes a similar phenotype (Jiang et al., 2004). Systemic administration of CXCL10 can reduce PF and inhibit the deposition of extracellular matrix by regulating angiogenesis (Jiang et al., 2010). Elevated *Cxcl10* expression in macrophages following hucMSCs infusion recruits Tregs into the lungs which may partially explain how hucMSCs perform their immunosuppressive function. *CXCR3* was also expressed in some alveolar type 2 cells (Ji et al., 2008), whose function remains to be investigated.

hucMSCs infusion does not affect the number of macrophages at the acute injury stage (Figure S4A-4B). However, there are decreased macrophage numbers at the fibrosis stage, and both alveolar macrophages and interstitial macrophages are decreased at the repair stage (Figure S4C-4F). Fewer macrophages lead to the decreased expression level of *Mrc1* (encode CD206) and *Chil3* (Fig. 3F and 3H), which play profibrotic roles during the repair phase. Administration of CD206 blocking peptide inhibits bleomycin-induced PF, which suggests that CD206 may be an interesting target for the treatment of fibrosis (Ghebremedhin et al., 2020). Chitinase 3-like 1 (coding by *Chil3*) is a prototypic chitinase-like protein that was elevated in patients with idiopathic PF(Lee et al., 2019; Zhou et al., 2014). In the bleomycin induce lung fibrosis model, *Chil3* expression was transiently decreased at the acute injury phase and then elevated at the fibrotic phase (Zhou et al., 2014). hucMSC infusion decreased macrophages at the fibrotic phase, which may also contribute to the alleviation of fibrosis caused by bleomycin.

PF is an important public health problem that leads to high mortality rates and an economic burden on patients. Here, we found that hucMSCs attenuated fibrosis induced by bleomycin and identified a subtype of interferon-sensitive macrophages. Our study suggests that hucMSCs perform immunosuppressive

functions by recruiting regulatory T cells, partially through their interaction with macrophages. Future investigations that combine single-cell RNA sequencing and *in vivo* tracing methods will clarify the mechanism of MSC in clinical models.

Conclusion

In the current study, we found hucMSCs can attenuate pulmonary fibrosis via macrophage. After hucMSC infusion, a subset of macrophage exhibited increased expression of interferon-responsive genes was identified by single cell RNA sequencing. This subtype of macrophages had increased *Cxcl10* expression that recruited more Tregs into the lung, which partially explains how the hucMSCs perform their immunosuppressive function.

Abbreviations

hucMSC: human umbilical mesenchymal stem cell; PF: pulmonary fibrosis; ECM: extracellular matrix; AM: alveolar macrophage; IM: interstitial macrophage; Treg: regulatory T cell; mGFP: membrane green fluorescent protein; IFNSM: IFN-sensitive macrophage; COVID-19: coronavirus disease 2019; SARS-CoV-2: severe acute respiratory syndrome coronavirus 2;

Declarations

Ethics approval and consent to participate

All experiments were performed in accordance with the recommendations of the Guide for Care and Use of Laboratory Animals of BeiKe Biotechnology. Ltd.

Consent for publication

Not applicable.

Availability of data and material

The datasets used and/or analyzed during the current study are available from the corresponding author on reasonable request.

Funding

National Key Research and Development Program of China (2018YFA0902703), Shenzhen KQTD project (KQTD20170331160605510), the Shenzhen Science and Technology Innovation Committee (JCYJ20180507182250795, JCYJ20170818164014753 and SY8A2211001), Key Project of Science and Technology helps economy (2020) of Guangdong province grant, and the National Natural Science Foundation of China (31800694 and 31971354).

Authors' contributions

Z.T., Y.H., M.Y.L, and N.L. conceived the experiments. J.X.G analyzed the sequencing data. Z.T., J.W., G.F.Z., Y.L., Z.K.S., and X.L. performed experiments and collected data. Z.T., J.X.G., J.Y.H., Y.H., M.Y.L., and N.L. analyzed the data and wrote the manuscripts. All authors read and approved the final manuscript.

Competing interests

The authors declare no competing interests.

Acknowledgements

Not applicable.

References

Aran, D., Looney, A.P., Liu, L., Wu, E., Fong, V., Hsu, A., Chak, S., Naikawadi, R.P., Wolters, P.J., Abate, A.R.*, et al.* (2019). Reference-based analysis of lung single-cell sequencing reveals a transitional profibrotic macrophage. Nat Immunol *20*, 163-172.

Atabai, K., Jame, S., Azhar, N., Kuo, A., Lam, M., McKleroy, W., Dehart, G., Rahman, S., Xia, D.D., Melton, A.C.*, et al.* (2009). Mfge8 diminishes the severity of tissue fibrosis in mice by binding and targeting collagen for uptake by macrophages. J Clin Invest *119*, 3713-3722.

Barkauskas, C.E., Cronce, M.J., Rackley, C.R., Bowie, E.J., Keene, D.R., Stripp, B.R., Randell, S.H., Noble, P.W., and Hogan, B.L. (2013). Type 2 alveolar cells are stem cells in adult lung. J Clin Invest *123*, 3025-3036.

Baumgartner, K.B., Samet, J.M., Stidley, C.A., Colby, T.V., and Waldron, J.A. (1997). Cigarette smoking: a risk factor for idiopathic pulmonary fibrosis. Am J Respir Crit Care Med *155*, 242-248.

Byrne, A.J., Maher, T.M., and Lloyd, C.M. (2016). Pulmonary Macrophages: A New Therapeutic Pathway in Fibrosing Lung Disease? Trends Mol Med *22*, 303-316.

Court, A.C., Le-Gatt, A., Luz-Crawford, P., Parra, E., Aliaga-Tobar, V., Batiz, L.F., Contreras, R.A., Ortuzar, M.I., Kurte, M., Elizondo-Vega, R.*, et al.* (2020). Mitochondrial transfer from MSCs to T cells induces Treg differentiation and restricts inflammatory response. EMBO Rep *21*, e48052.

Dancer, R.C., Wood, A.M., and Thickett, D.R. (2011). Metalloproteinases in idiopathic pulmonary fibrosis. Eur Respir J *38*, 1461-1467.

Downey, G.P. (2011). Resolving the scar of pulmonary fibrosis. N Engl J Med *365*, 1140-1141.

Galleu, A., Riffo-Vasquez, Y., Trento, C., Lomas, C., Dolcetti, L., Cheung, T.S., von Bonin, M., Barbieri, L., Halai, K., Ward, S.*, et al.* (2017). Apoptosis in mesenchymal stromal cells induces in vivo recipient-mediated immunomodulation. Sci Transl Med *9*.

Ghebremedhin, A., Salam, A.B., Adu-Addai, B., Noonan, S., Stratton, R., Ahmed, M.S.U., Khantwal, C., Martin, G.R., Lin, H., Andrews, C.*, et al.* (2020). A Novel CD206 Targeting Peptide Inhibits Bleomycin Induced Pulmonary Fibrosis in Mice. bioRxiv.

Groom, J.R., and Luster, A.D. (2011). CXCR3 in T cell function. Exp Cell Res *317*, 620-631.

Ji, R., Lee, C.M., Gonzales, L.W., Yang, Y., Aksoy, M.O., Wang, P., Brailoiu, E., Dun, N., Hurford, M.T., and Kelsen, S.G. (2008). Human type II pneumocyte chemotactic responses to CXCR3 activation are mediated by splice variant A. Am J Physiol Lung Cell Mol Physiol *294*, L1187-1196.

Ji, W.J., Ma, Y.Q., Zhou, X., Zhang, Y.D., Lu, R.Y., Sun, H.Y., Guo, Z.Z., Zhang, Z., Li, Y.M., and Wei, L.Q. (2014). Temporal and spatial characterization of mononuclear phagocytes in circulating, lung alveolar and interstitial compartments in a mouse model of bleomycin-induced pulmonary injury. J Immunol Methods *403*, 7-16.

Jiang, D., Liang, J., Campanella, G.S., Guo, R., Yu, S., Xie, T., Liu, N., Jung, Y., Homer, R., Meltzer, E.B.*, et al.* (2010). Inhibition of pulmonary fibrosis in mice by CXCL10 requires glycosaminoglycan binding and syndecan-4. J Clin Invest *120*, 2049-2057.

Jiang, D., Liang, J., Hodge, J., Lu, B., Zhu, Z., Yu, S., Fan, J., Gao, Y., Yin, Z., Homer, R.*, et al.* (2004). Regulation of pulmonary fibrosis by chemokine receptor CXCR3. J Clin Invest *114*, 291-299.

Jun, D., Garat, C., West, J., Thorn, N., Chow, K., Cleaver, T., Sullivan, T., Torchia, E.C., Childs, C., Shade, T.*, et al.* (2011). The pathology of bleomycin-induced fibrosis is associated with loss of resident lung mesenchymal stem cells that regulate effector T-cell proliferation. Stem Cells *29*, 725-735.

Karin, N., and Razon, H. (2018). Chemokines beyond chemo-attraction: CXCL10 and its significant role in cancer and autoimmunity. Cytokine *109*, 24-28.

Ko, J.H., Kim, H.J., Jeong, H.J., Lee, H.J., and Oh, J.Y. (2020). Mesenchymal Stem and Stromal Cells Harness Macrophage-Derived Amphiregulin to Maintain Tissue Homeostasis. Cell Rep *30*, 3806-3820 e3806.

Kopf, M., Schneider, C., and Nobs, S.P. (2015). The development and function of lung-resident macrophages and dendritic cells. Nat Immunol *16*, 36-44.

Lee, C.M., He, C.H., Park, J.W., Lee, J.H., Kamle, S., Ma, B., Akosman, B., Cotez, R., Chen, E., Zhou, Y.*, et al.* (2019). Chitinase 1 regulates pulmonary fibrosis by modulating TGF-beta/SMAD7 pathway via TGFBRAP1 and FOXO3. Life Sci Alliance *2*.

Lee, S.H., Jang, A.S., Kim, Y.E., Cha, J.Y., Kim, T.H., Jung, S., Park, S.K., Lee, Y.K., Won, J.H., Kim, Y.H.*, et al.* (2010). Modulation of cytokine and nitric oxide by mesenchymal stem cell transfer in lung injury/fibrosis. Respir Res *11*, 16.

Li, W., Chen, W., Huang, S., Yao, G., Tang, X., and Sun, L. (2020). Mesenchymal stem cells prevent overwhelming inflammation and reduce infection severity via recruiting CXCR3(+) regulatory T cells. Clin Transl Immunology *9*, e1181.

Liu, T., Ullenbruch, M., Young Choi, Y., Yu, H., Ding, L., Xaubet, A., Pereda, J., Feghali-Bostwick, C.A., Bitterman, P.B., Henke, C.A.*, et al.* (2013). Telomerase and telomere length in pulmonary fibrosis. Am J Respir Cell Mol Biol *49*, 260-268.

Mansouri, N., Willis, G.R., Fernandez-Gonzalez, A., Reis, M., Nassiri, S., Mitsialis, S.A., and Kourembanas, S. (2019). Mesenchymal stromal cell exosomes prevent and revert experimental pulmonary fibrosis through modulation of monocyte phenotypes. JCI Insight *4*.

Martinez, F.J., Collard, H.R., Pardo, A., Raghu, G., Richeldi, L., Selman, M., Swigris, J.J., Taniguchi, H., and Wells, A.U. (2017). Idiopathic pulmonary fibrosis. Nat Rev Dis Primers *3*, 17074.

Misharin, A.V., Morales-Nebreda, L., Mutlu, G.M., Budinger, G.R., and Perlman, H. (2013). Flow cytometric analysis of macrophages and dendritic cell subsets in the mouse lung. Am J Respir Cell Mol Biol *49*, 503-510.

Moodley, Y., Atienza, D., Manuelpillai, U., Samuel, C.S., Tchongue, J., Ilancheran, S., Boyd, R., and Trounson, A. (2009). Human umbilical cord mesenchymal stem cells reduce fibrosis of bleomycin-induced lung injury. Am J Pathol *175*, 303-313.

Morrison, T.J., Jackson, M.V., Cunningham, E.K., Kissenpfennig, A., McAuley, D.F., O'Kane, C.M., and Krasnodembskaya, A.D. (2017). Mesenchymal Stromal Cells Modulate Macrophages in Clinically Relevant Lung Injury Models by Extracellular Vesicle Mitochondrial Transfer. Am J Respir Crit Care Med *196*, 1275-1286.

Ono, M., Ohkouchi, S., Kanehira, M., Tode, N., Kobayashi, M., Ebina, M., Nukiwa, T., Irokawa, T., Ogawa, H., Akaike, T.*, et al.* (2015). Mesenchymal stem cells correct inappropriate epithelial-mesenchyme relation in pulmonary fibrosis using stanniocalcin-1. Mol Ther *23*, 549-560.

Ortiz, L.A., Gambelli, F., McBride, C., Gaupp, D., Baddoo, M., Kaminski, N., and Phinney, D.G. (2003). Mesenchymal stem cell engraftment in lung is enhanced in response to bleomycin exposure and ameliorates its fibrotic effects. Proc Natl Acad Sci U S A *100*, 8407-8411.

Sanchez-Guijo, F., Garcia-Arranz, M., Lopez-Parra, M., Monedero, P., Mata-Martinez, C., Santos, A., Sagredo, V., Alvarez-Avello, J.M., Guerrero, J.E., Perez-Calvo, C.*, et al.* (2020). Adipose-derived mesenchymal stromal cells for the treatment of patients with severe SARS-CoV-2 pneumonia requiring mechanical ventilation. A proof of concept study. EClinicalMedicine *25*, 100454.

Sheng, G., Chen, P., Wei, Y., Yue, H., Chu, J., Zhao, J., Wang, Y., Zhang, W., and Zhang, H.L. (2020). Viral Infection Increases the Risk of Idiopathic Pulmonary Fibrosis: A Meta-Analysis. Chest *157*, 1175-1187.

Sisson, T.H., Mendez, M., Choi, K., Subbotina, N., Courey, A., Cunningham, A., Dave, A., Engelhardt, J.F., Liu, X., White, E.S.*, et al.* (2010). Targeted injury of type II alveolar epithelial cells induces pulmonary fibrosis. Am J Respir Crit Care Med *181*, 254-263.

Strieter, R.M., Gomperts, B.N., and Keane, M.P. (2007). The role of CXC chemokines in pulmonary fibrosis. J Clin Invest *117*, 549-556.

Tager, A.M., Kradin, R.L., LaCamera, P., Bercury, S.D., Campanella, G.S., Leary, C.P., Polosukhin, V., Zhao, L.H., Sakamoto, H., Blackwell, T.S.*, et al.* (2004). Inhibition of pulmonary fibrosis by the chemokine IP-10/CXCL10. Am J Respir Cell Mol Biol *31*, 395-404.

Tan, S.Y., and Krasnow, M.A. (2016). Developmental origin of lung macrophage diversity. Development *143*, 1318-1327.

Wu, H., Yu, Y., Huang, H., Hu, Y., Fu, S., Wang, Z., Shi, M., Zhao, X., Yuan, J., Li, J.*, et al.* (2020). Progressive Pulmonary Fibrosis Is Caused by Elevated Mechanical Tension on Alveolar Stem Cells. Cell *180*, 107-121 e117.

Wynn, T.A., and Vannella, K.M. (2016). Macrophages in Tissue Repair, Regeneration, and Fibrosis. Immunity *44*, 450-462.

Xie, T., Wang, Y., Deng, N., Huang, G., Taghavifar, F., Geng, Y., Liu, N., Kulur, V., Yao, C., Chen, P.*, et al.* (2018). Single-Cell Deconvolution of Fibroblast Heterogeneity in Mouse Pulmonary Fibrosis. Cell Rep *22*, 3625-3640.

Yao, C., Guan, X., Carraro, G., Parimon, T., Liu, X., Huang, G., Mulay, A., Soukiasian, H.J., David, G., Weigt, S.S.*, et al.* (2021). Senescence of Alveolar Type 2 Cells Drives Progressive Pulmonary Fibrosis. Am J Respir Crit Care Med *203*, 707-717.

Zhou, Y., Peng, H., Sun, H., Peng, X., Tang, C., Gan, Y., Chen, X., Mathur, A., Hu, B., Slade, M.D.*, et al.* (2014). Chitinase 3-like 1 suppresses injury and promotes fibroproliferative responses in Mammalian lung fibrosis. Sci Transl Med *6*, 240ra276.

Figures

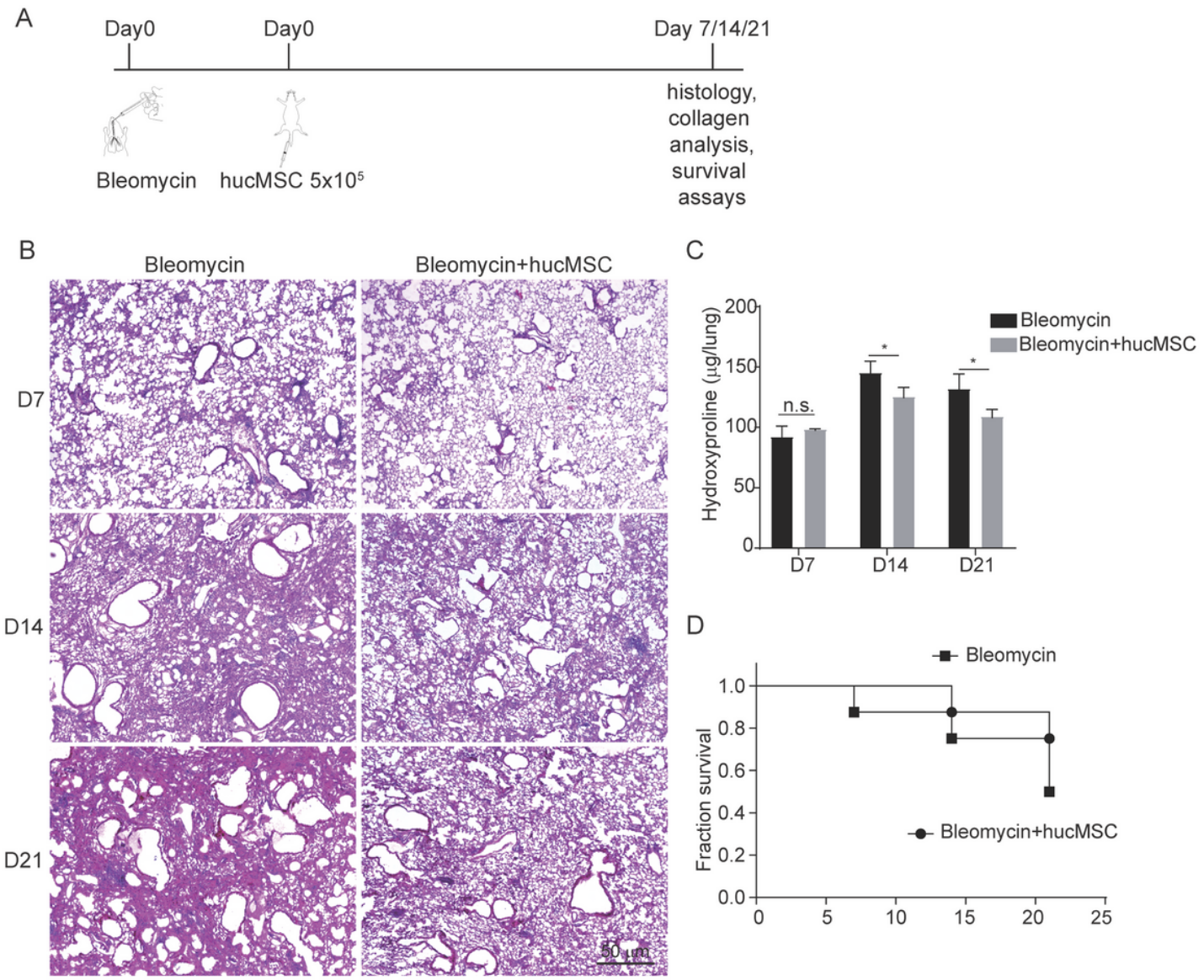

Figure 1

hucMSCs alleviated bleomycin-induced pulmonary fibrosis (A) Scheme of the experimental timeline for the bleomycin-induced pulmonary fibrosis model and hucMSCs infusion. (B) H&E-stained lung sections from bleomycin-treated mice and hucMSC-treated mice at various time points. (C) Hydroxyproline contents of bleomycin-treated mice lung and hucMSC-treated mice lungs at various time points (mean ± S.D, n=3 mice per group). (D) Survival curves of bleomycin-treated mice and hucMSC-treated mice (n=12 mice per group). *p < 0.05, Student's t-test.

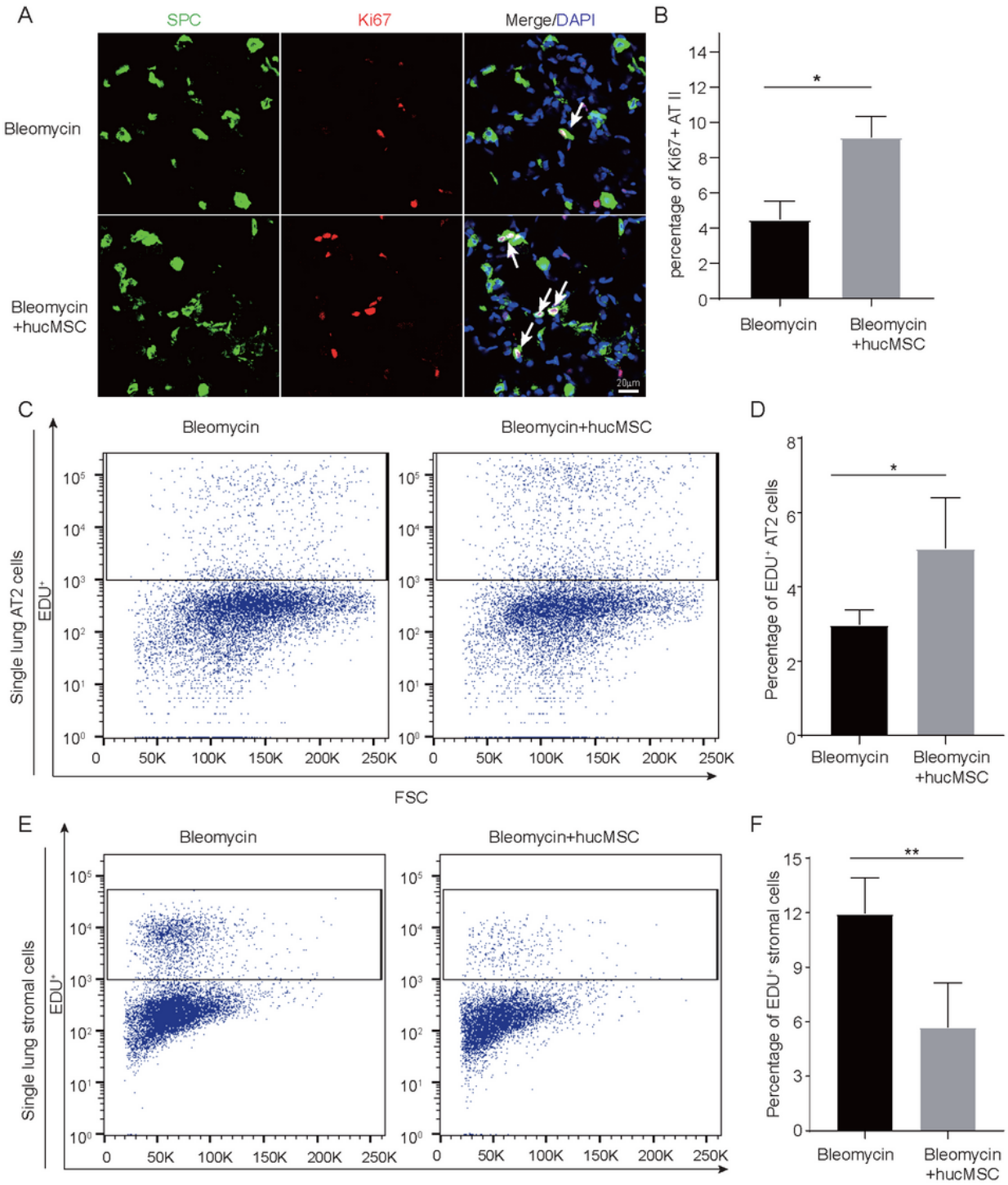

Figure 2

hucMSCs infusion promoted lung regeneration (A) Day 7 after bleomycin treatment, lung sections were stained with antibodies against proSPC and Ki67. White arrowheads indicate proliferating alveolar type 2 cells. (B) The percentage of Ki67-positive alveolar type 2 cells (mean ± S.D, n=3 mice per group). (C) Flow cytometry analysis of EdU incorporation in alveolar type 2 cells in bleomycin-treated mice lungs and hucMSCs treated mice lungs on day 7. (D) The percentage of EdU-positive alveolar type 2 cells (mean ±

S.D, n=3 mice per group). (E) Flow cytometry analysis of EdU incorporation in lung fibroblast cells in bleomycin-treated mice lungs and hucMSCs treated mice lungs on day 7. (F) The percentage of EdU-positive lung fibroblast cells (mean ± S.D, n=3 mice per group). *p < 0.05, **p < 0.05, Student's t-test.

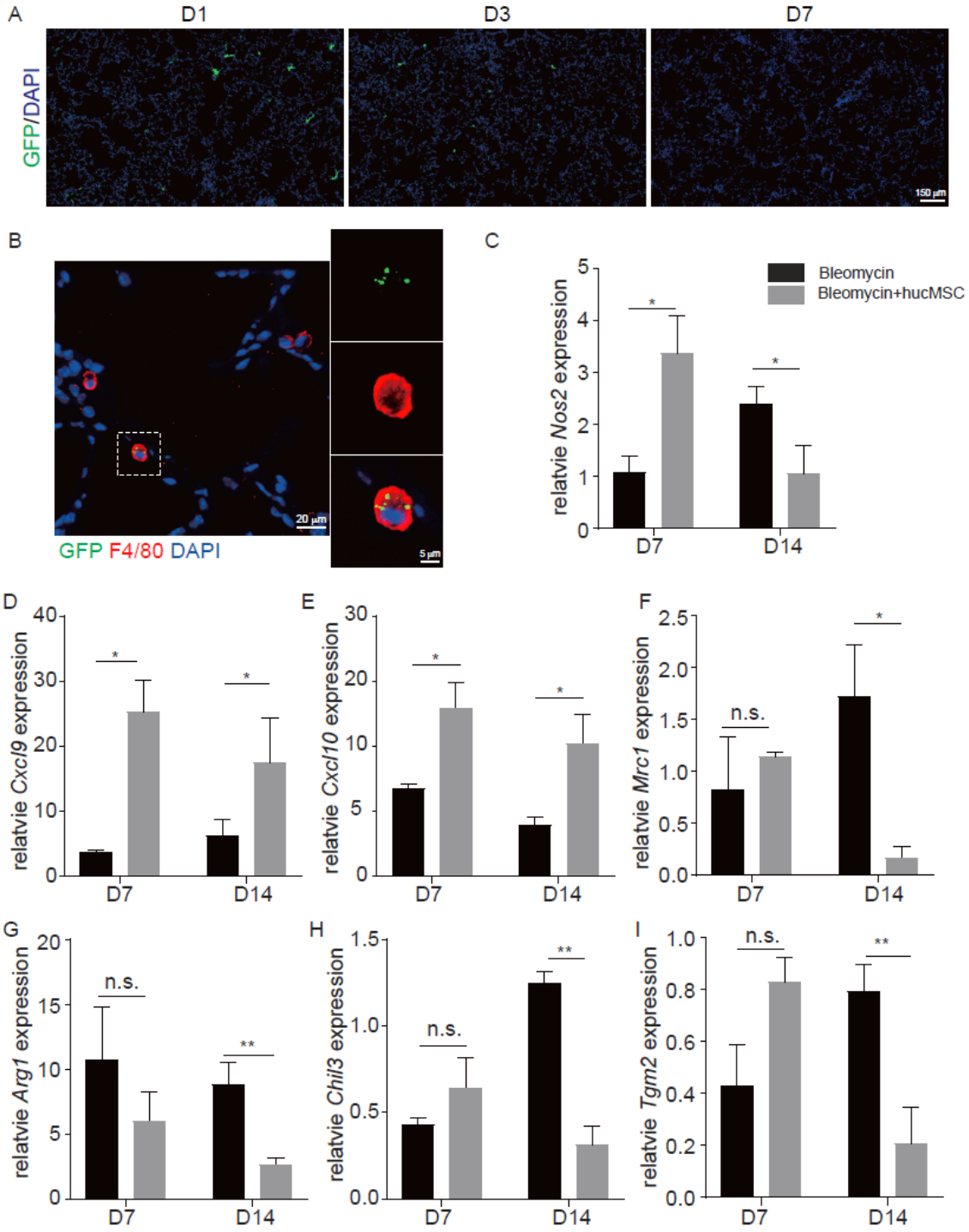

Figure 3

hucMSCs interacted with macrophages after infusion (A) Immunofluorescent labeling of lung sections after GFP-labeled hucMSCs infusion in bleomycin-treated lungs at various time points. (B) Lung sections

were stained with antibodies against GFP and F4/80. (C-l) Nos2, Cxcl9, Cxcl10, Mrc1, Arg1, Chil3, and Tgm2 expression levels in bleomycin-treated lungs and hucMSCs treated lungs on day 7 and day 14 by whole lung qRT-PCR. Nos2, Cxcl9, and Cxcl10 expression levels (mean ± S.D, n=3 mice per group) were significantly increased in hucMSCs treated lungs compared to bleomycin-treated lungs at day 7 (C-E). Mrc1, Arg1, Chil3, and Tgm2 expression levels (mean ± S.D, n=3 mice per group) were significantly decreased in hucMSCs treated lungs compared to bleomycin-treated lungs at day 14 (F-l). *p < 0.05, **p < 0.01, n.s. no significant difference, Student's t-test.

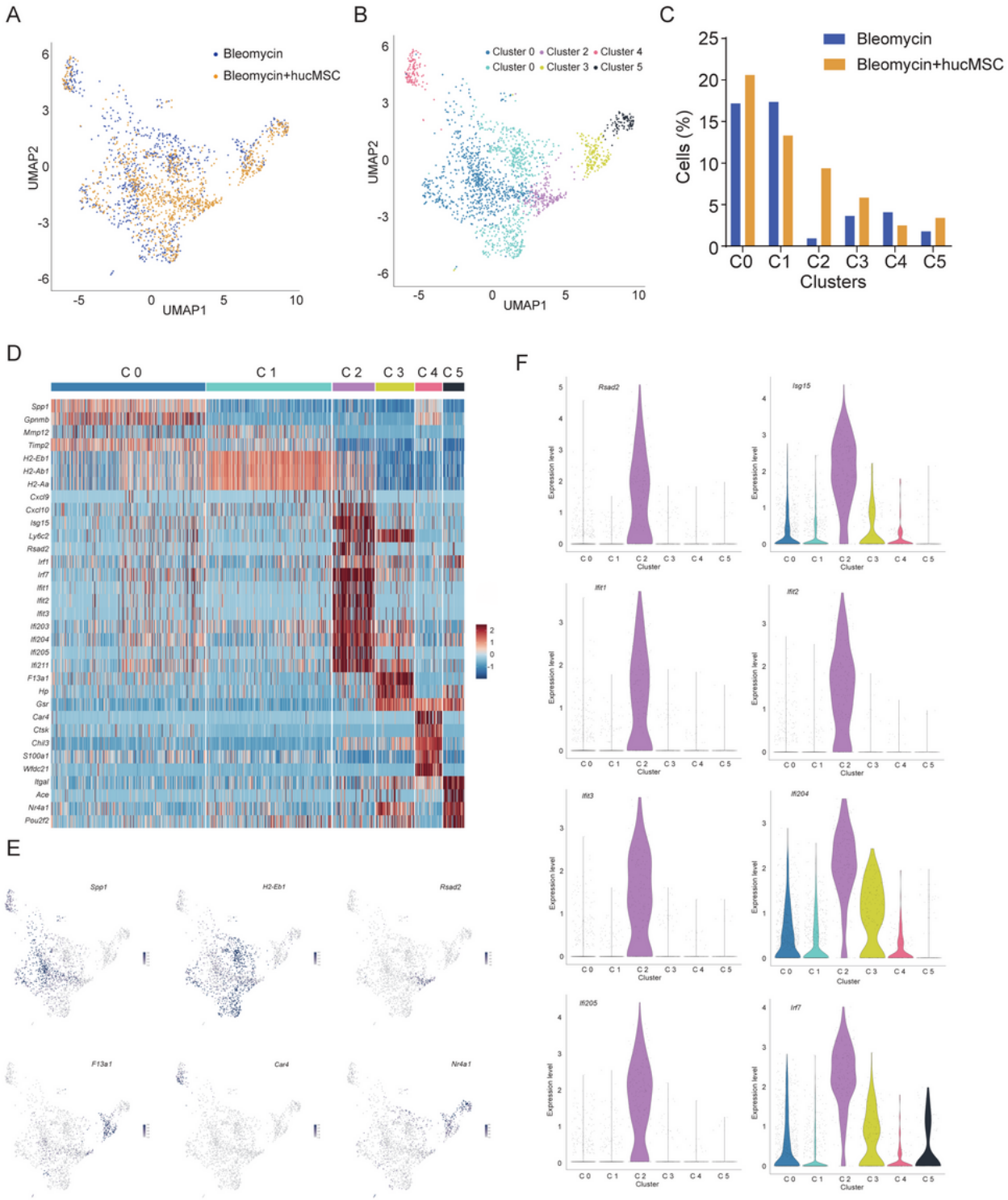

Figure 4

Single-cell RNA sequencing revealed an interferon-sensitive macrophage population in hucMSCs infused lungs (A) UMAP plot of macrophages from bleomycin- and hucMSCs treated mouse lungs. (B and C) The proportions of different macrophage clusters. (D) Heatmap of some differentially expressed genes between each macrophage cluster. (E) t-SNE visualization overlaid with the expression of Spp1, H2-Eb1, Rsad2, F13a1, Car4, and Nr4a1. (F) Violin plots of Rsad2, Isg15, Ifit1, Ifit2, Ifit3, Ifi204, Ifi205, and Irf7 expression in each macrophage cluster.

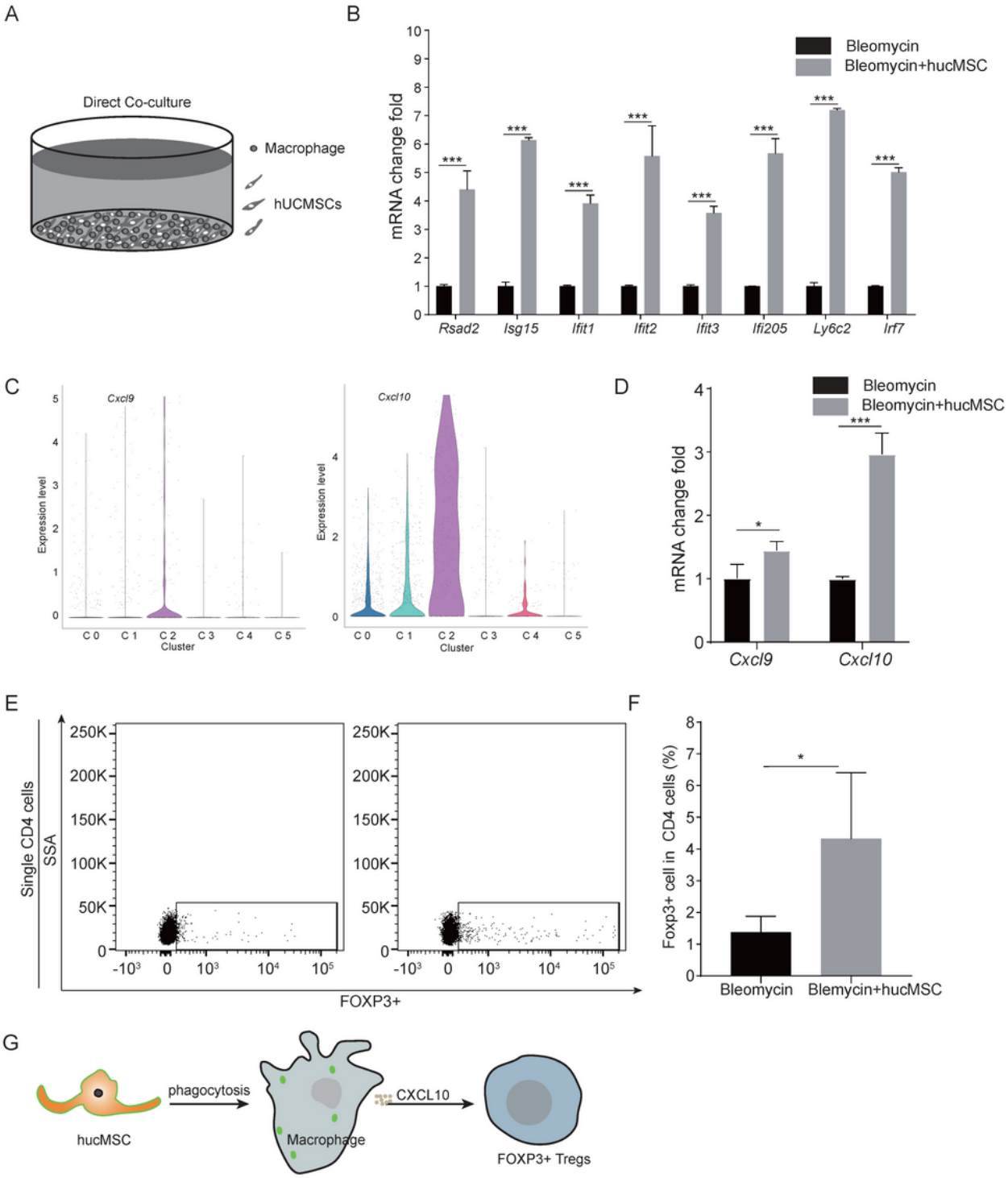

Figure 5

Macrophage and hucMSCs interaction increased interferon responsive gene expression in macrophages (A) Diagram of macrophage and hucMSCs co-culture. (B) Rsad2, Isg15, Ifit1, Ifit2, Ifit3, Ifi204, Ifi205, and Irf7 expression levels in macrophage co-cultured hucMSCs (mean ± S.D, n=3 wells per group). (C) Violin plots of Cxcl9 and Cxcl10 in each macrophage cluster. (D) Cxcl9 and Cxcl10 expression levels in macrophages co-cultured with hucMSCs (mean ± S.D, n=3 wells per group). (E) Flow cytometry analysis of Foxp3 regulatory T cells in bleomycin-treated mice lungs and hucMSCs treated mice lung. (F) Quantification of Foxp3 positive Tregs in bleomycin-treated mice lungs and hucMSCs treated mice lungs at day 7 (mean ± S.D, n=3 mice per group). *p < 0.05, ***p < 0.001, n.s. no significant difference, Student's t-test.

Supplementary Files

This is a list of supplementary files associated with this preprint. Click to download.

- FigS1.png
- FigS2.png
- FigS3.png
- FigS4.png